Int J Coal Sci Technol (2016) 3(4):418–428
DOI 10.1007/s40789-016-0153-y

Changes in organic structure and mineral phases transformation of coal during heat treatment on laboratory scale

Vivek Mishra[1] · Mamta Sharma[1] · Sanchita Chakravarty[1] · Amit Banerjee[1]

Received: 3 June 2016 / Revised: 30 November 2016 / Accepted: 8 December 2016 / Published online: 22 December 2016

Abstract Structural changes due to coalification and oxidation influence the coal quality, geochemically and petrologically. Understanding of the coal structures helps to predict the behaviour of coal at various processes. The objective of this paper is to study the changes in organic structure and mineral phase transformation during combustion. Different density fractions were generated and then heated at different temperatures from 200 to 1000 °C. Petrography, Fourier transform infrared spectroscopy (FTIR) and X-ray diffraction (XRD) were carried out on all the density fractions aimed to accomplish this objective. Here, through petrography, it was observed that the vitrinite and liptinite macerals disappear at higher temperature while porous inertinite is seen. The inertinite structure is exposed which is assumed by the presence of −OH and C–O–C stretches with the aromatic nucleus (CH) and three to four adjacent H from FTIR spectra. Moreover, it can be concluded that aliphatic groups get collapsed at high temperature. In case of inorganic matter, through XRD and FTIR, it is also revealed that with increasing temperature, clay minerals converted into elemental oxides. Hence, this study is suggesting that the structures of coal are altered by the degree of contact metamorphism.

Keywords Coal · Heat treatment · Oxidation · Petrography · FTIR · XRD

1 Introduction

Coal consists of primary macromolecules of polyaromatic-polynuclear structure with some heteroatom groups and their secondary networks, latter of which are derived from aromatic ring stacking, aliphatic side chain entanglement, and hydrogen bonds, cation bridges, charge-transfer interactions through oxygen functional groups (Solum et al. 1989; Carlson 1992; Cody et al. 1993; Nakamura et al. 1995; Larsen et al. 1996; Wu et al. 2013). The oxidation of coal is a complex and multifaceted process representing a perplexing issue for both scientists and industrialist alike. The scientist seeks to understand the physical and chemical transformations brought about by oxidation, whereas the changes in behaviour specific to a given technological processes is the dominant concern of industry. Because oxidation alters the surface characteristics of both coal and mineral particles, flotation efficiencies may be changed and coal cleaning characteristics degraded (Sun 1954; Taylor et al. 1980). Conversely, mild, low temperature oxidation affects the process of gasification, reduces the caking tendencies and increases char reactivity (Mahajan et al. 1980). Hence, changes in behaviour may relate to changes in operating cost (Lowcnhaupt and Gray 1980) and there is a need to determine the extent of oxidation.

Coal undergoes structural changes when heated to a temperature at which thermal decomposition occurs (Ozbas and Kok 2003; Acma et al. 2006; Giroux et al. 2006). Fully characterizing coal structures is still a challenging issue due to the heterogeneity, non-crystalline structure, and insolubility of coal. Inertinite is the most aromatic and most thermally stable of all the maceral groups (Pandolfo et al. 1988; White et al. 1989; Vasallo et al. 1991; Xie et al. 1991; Sun et al. 2003; Wang et al. 2010). In this group, the

✉ Vivek Mishra
vmishrageology@gmail.com

[1] CSIR – National Metallurgical Laboratory, Jamshedpur 831007, India

maceral fusinite is more aromatic than semifusinite from the same coal (Blanc et al. 1991; Diessel 1992; Morga 2010). On the other hand, the amount of mobile hydrogen is higher in semifusinite than in fusinite (Maroto-Valer et al. 1998).

In this work, the compositional and structural changes that occur as a consequence of heat treatment of a bituminous coal performed at 200–1000 °C were investigated qualitatively. The study has been undertaken to develop a better understanding of the effect that the variations of mineralogical compositions, as a result of smouldering, have on the technological properties important for coal utilisation. The effect of heat treatment on the organic matrix of the coal has been discussed in detail. The results obtained would throw light not only on the nature and on distribution of organic matter (macerals) but also on the types of mineralogical transformations, which can take place during heating. As coal is heated, the inorganic phases undergo transformations and reactions that yield a complex mixture of solid, molten, and volatile species. There are many different minerals that behave differently. The main refractory minerals are quartz, metakaolinite, mullite, and rutile, while the common fluxing minerals are anhydrite, acid plagioclases, Kfeldspars, Ca silicates, and hematite (Vassileva and Vassilev 2006; Creelman et al. 2013; Mishra et al. 2016).

Chemical structure of coal macerals can be well examined by means of FTIR spectroscopy which makes it possible to obtain good quality spectra even from relatively small grains (Painter et al. 1978, 1980, 1981a, b; Bouwman and Freriks 1980; Painter and Rhoads 1981; Solomon 1981; Kuehn et al. 1982; Meyer 1982; Solomon and Carangelo 1982, 1988; Mastalerz and Bustin 1993a, b, 1995, 1996; Guo and Bustin 1998; Bustin and Guo 1999; Walker and Mastalerz 2004; Singh et al. 2015). Therefore, Fourier transform infrared spectroscopy (FTIR) is used as a physical detection technique and is widely applied in characterizing the chemical structures of coal. Besides, to quantify the mineralogical transformation X-ray diffraction analysis (XRD) analysis has been done on the samples.

2 Experimental section

2.1 Sampling and preparation of coal

Samples were taken from Jamadoba colliery (Fig. 1) of Jharia coalfield. The stratigraphy (Table 1) of Jharia coalfield unconformably overlies the Archean basement and belongs to the Lower Gondwana of Permian age. The stratigraphic succession in the coalfield comprises Talchir,

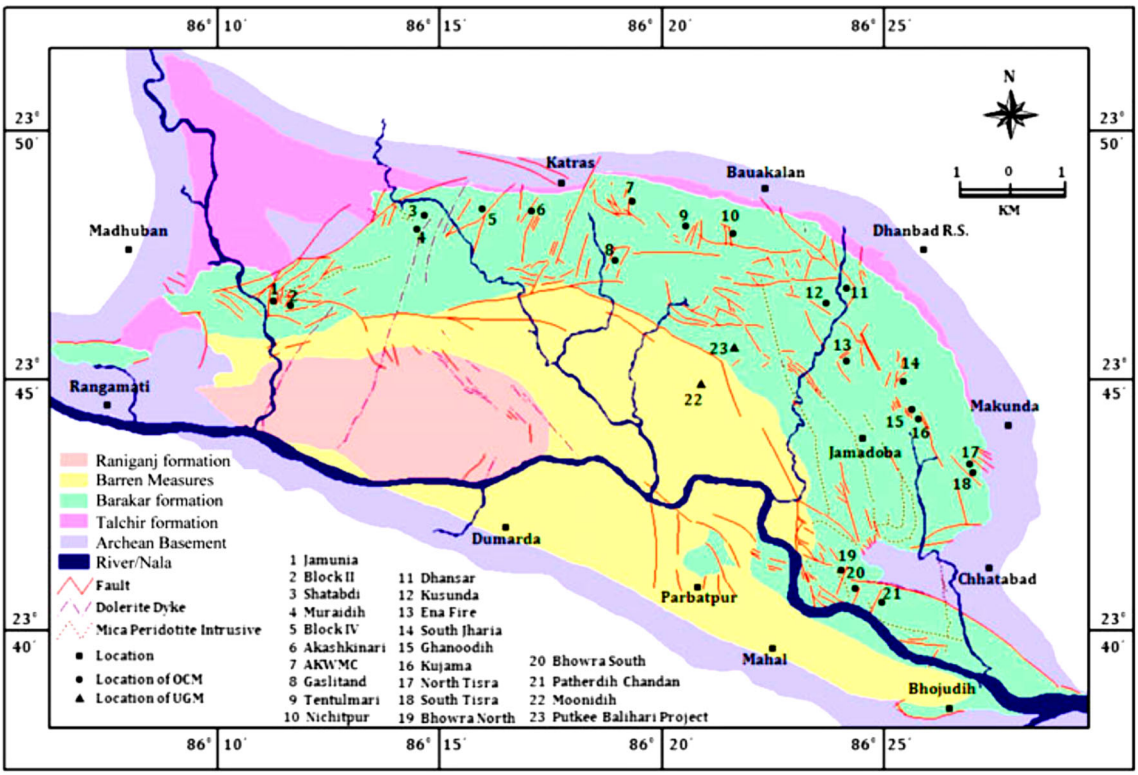

Fig. 1 Geological map of the study area (modified after Paul and Chatterjee 2011)

Table 1 Generalised stratigraphic succession of Jharia coalfield (modified after Chandra 1992)

Age	Formation	Litho-type	Max. thickness (m)
Recent and sub-recent	Weathered	Alluvium, sandy soil, clay, gravel, etc.	30
Unconformity			
Jurassic	Deccan trap and other igneous activity (intrusive)	Dolerite dykes, mica lamprophyre dyke and sills	
Upper Permian	Raniganj	Fine grained feldspathic sandstones, shales with coal seam	800
Middle Permian	Barren measure	Buff coloured sandstone, shales and carbonaceous shales	730
Lower Permian	Barakar	Buff coloured coarse to medium grained feldspathic sandstones, grits, shales, carbonaceous shale and coal seam	+1250
Upper Carboniferous	Talchir	Greenish shale and fine grained sandstones	245
Archeans	Metamorphics		

Table 2 Proximate and ultimate analysis of representative coal samples with yield % obtained in float fraction of different densities

Sample	Yield (%)	Proximate analysis				Ultimate analysis			
		M_a	VM_{daf}	A_d	FC_{daf}	C_{daf}	H_{daf}	N_{daf}	S_{daf}
HS		1.57	24.04	19.00	75.96	74.41	3.07	1.25	0.57
F1.3	2.5	1.66	24.00	10.04	76.00	80.76	4.19	1.36	0.83
F1.4	17.8	1.37	21.72	19.54	78.28	72.71	3.62	1.21	0.65
F1.5	39.3	1.32	22.69	32.27	77.31	58.67	3.18	1.11	0.61

HS Head Sample, *M* Moisture, *VM* Volatile Matter yield (wt%), *A* Ash yield (wt%), *F.C.* Fixed carbon (wt%), *C* Carbon (wt%), *H* Hydrogen (wt%), *N* Nitrogen (wt%), *S* Sulphur (wt%), *a* analytical state, *d* dry basis, *daf* dry ash free basis

Barakar, Barren measures and Raniganj formations, from bottom to top (Fox 1934; Mehta and Murthy 1957).

The collected sample was used for laboratory thermal alteration, which was performed at different temperatures. The sample was crushed, pulverized, and passed through 3 mm sieve. −3 mm size fraction weighing 1 kg was followed to heavy media separation with the relative density range from 1.3 to 1.5 gm/cm^3, made by benzene (density: 0.8 gm/cm^3) and bromoform (density: 2.8 gm/cm^3) mixture, for heat treatment study. Thus, from a single sample, three different density samples were prepared and 5 gm of each density fractions were heated at 200, 400, 600, 800 and 1000 °C temperatures at oxidizing atmosphere for a period of 1 h to attain the temperature of 1000 °C. After that, the furnace was cooled at the rate of 6 °C/min. Beyond 1000 °C, coal is reduced into ash and the organic matter is completely burnt.

2.2 Proximate and ultimate analysis

Proximate and ultimate analysis of the representative and their fractionated coal samples were carried out in the coal characterisation laboratory using standard analytical procedures. The proximate analysis was performed taking 72 mesh size coal powder using oven and muffle furnace as per Bureau of Indian Standard (BIS 2003). The elemental analysis (C, H, N and S) was performed using Vario EL III CHNS analyser (Elementar GmbH, Germany).

2.3 Petrography, XRD and FTIR

To study the coal samples under microscope the samples were crushed and passed through −18 mesh size and pellets were prepared in cold medium of epoxy-resin and hardener. The maceral analysis was carried out on polished mounts of coal with a polarized transmitted microscope having fluorescence attachment (Leica DM4500P) using established ICCP (1963, 1998, 2001) recommendations.

Mineralogical analysis of the coal samples were performed by means of X-ray diffraction (XRD) with Ni-filtered CuKα radiation at (10°–70°)/(2θ) at a scan rate of 2°/min (D8 Discover Bruker) using High Score Plus software package to obtain quantitative mineral proportion.

IR spectra of the samples were recorded with a Perkin–Elmer (model-Paragon 500) FT-IR spectrometer in the range of 4000–400 cm^{-1} on KBr pellet.

3 Result and discussion

3.1 Proximate and ultimate

Table 2 reveals the general characteristics of the head sample and the prepared samples from heavy media separation. The yield % of the float fractions of different densities are also tabulated there. The volatile matter (VM_{daf}) and ash yields (A_d) are 24.04 and 19.0 wt% respectively. In the fractions, *VM* and moisture are decreasing with density while ash is increasing. Carbon, hydrogen, nitrogen and sulphur, all are also decreasing with density.

3.2 Organic change from petrography and FTIR

3.2.1 Petrography

All the coal samples prepared by heating in an oxidising condition at different temperatures from 200 to 1000 °C were subjected to petrography to study the heating-induced changes in micro-texture and structure of coal (Fig. 2; Table 3). The percentage of inertinite macerals increased with density in all the temperatures while the macerals which were affected by heat (heat affected maceral), seen to increase with density at only 200 °C. These two components decreased with density in the samples treated at other temperature range (400–1000 °C). Oxidised macerals were only found in 400 °C where it also decreased with density. The mean reflectance of vitrinite macerals increased with temperature (≤400 °C) and density both. Vitrinites were seen below 600 °C since it was totally transformed into heat affected macerals at higher temperature. The mineral matter relatively increased with density at all temperature ranges.

Table 4, shows the IR spectra of macerals. The major FTIR spectra of vitrinite are the aromatic C=C ring stretching vibration at 1615–1585 cm^{-1}, aliphatic absorption at 1460–1450 and 3000–2800 cm^{-1}. Weak peaks occur at 1740–1700 cm^{-1} due to C=O group absorption, and at 3050–3030 cm^{-1}, due to aromatic CH*x* stretching vibration (Xuguang 2005). In our coal, all the three major peaks were identified. 3039–2916 and 1603–1575 cm^{-1} are present below 600 °C which is in a perfect match with petrography where vitrinite is not found above 400 °C. The strongest aromatic C=C ring stretching at 1600 cm^{-1}, and the weakest aliphatic CH*x* stretching at 3000–2800 cm^{-1}, establishes the fact that fusinite has the highest degree of aromatic substituents and condensation of aromatic rings, and aliphatic substances is minor (Xuguang 2005). Thermal stability of inertinite macerals are higher than the other macerals probably due to its aromatic nature (Sun et al. 2003; Wang et al. 2010; Roberts et al. 2015). In our coal, the presence of inertinite found throughout the whole temperature range (200–1000 °C).

Fig. 2 Photomicrograph of laboratory oxidative alteration of some of the macerals from Jamadoba coals (**A1**). Telovitrinite, semifusinite and inertodetrinite (**A2**). Detrovitrinite and fusinite (**A3**). Semifusinite is filled by clay (**A4**). Fusinite with macrinite and low reflectivity semifusinite sample, thermally activated cracks (**B1**). Thermally activated cracks with oxidised semifusinite (**B2**). Low reflective semifusinite surrounded by oxidised bright semifusinite (**B3**), Fusinite (**B4**). The oxidation of semifusinite is started from the grain boundary. Centre part of grain is almost not metamorphosed with fragments of inertodetrinite (**B5**). Thermally altered of detrovitrinite, Inertodetrinite, heat affected (**C1**). Heat affected inertinite filled by mineral matter (**C2**). Fusinite with pores increasing in size due to heat (**C3**). Mineral matter with trace amount of fusinite (**D1**). Quartz and siderite (**D2**). Highly metamorphosed fusinite (**E1**), Quartz (**E2**). Altered coal with showing character of coke with many macropores ▶

At 200 °C (Fig. 2**A1**–**A4**), the mean reflectance of vitrinite (Table 3) increased with density but did not show any change in the maceral and microtextural constituents. Telovitrinite, detrovitrinite, were observed in vitrinite group maceral. In case of inertinite group macerals, fusinite is low in concentration than semifusinite. Inertodetrinite is also seen in the float fractions of the density of 1.3 gm/cm^3. Among liptinite group meceral, resinite is seen in this density but in low concentration. The clay minerals are associated with semifusinite. In the float fractions of the density of 1.4, telovitrinites were observed and the inertinite macerals were dominated by semifusinite. Fusinite and macrinite occur in low concentration. In the float fractions of density of 1.5, the dominated macerals are detrovitrinite and semifusinite. Low reflectivity of semifusinite is observed in all density fractions at this temperature.

At 400 °C (Fig. 2**B1**–**B5**) temperature, the sub-macerals of vitrinite and inertinite are oxidised in all density fractions. In the float fractions of the density of 1.3, telovitrinite, semifusinite and inertodetrinite were observed. Thermally activated cracks were developed in semifusinite. In float fractions of the density of 1.4, fusinite and semifusinite were seen. The reflectivity of semifusinite was changed in this temperature and this oxidation was started from grain boundaries. Thus low reflective semifusinite, surrounded by bright semifusinite, found at this temperature. Thermally altered detrovitrinite, inertodetrinite, heat affected macerals were also observed. In float fractions of the density of 1.5, detrovitrinite and inertodetrinite were seen. Heat affected macerals were found in very low amount in this density. Oxidised macerals were observed at this temperature range (>200 °C, <600 °C). Beyond this

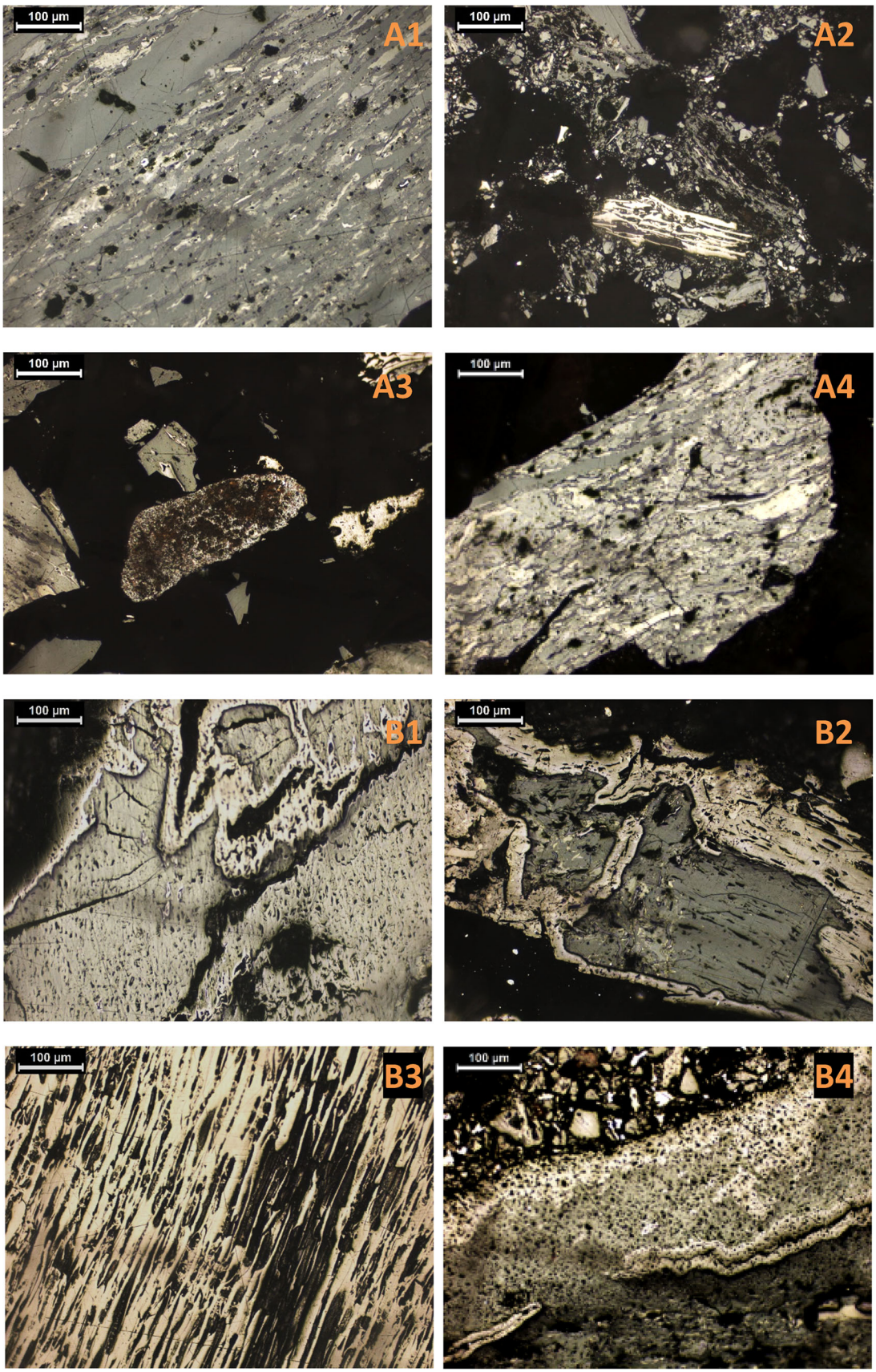
100 µm
A1
100 µm
A2
100 µm
A3
100 µm
A4
100 µm
B1
100 µm
B2
100 µm
B3
100 µm
B4

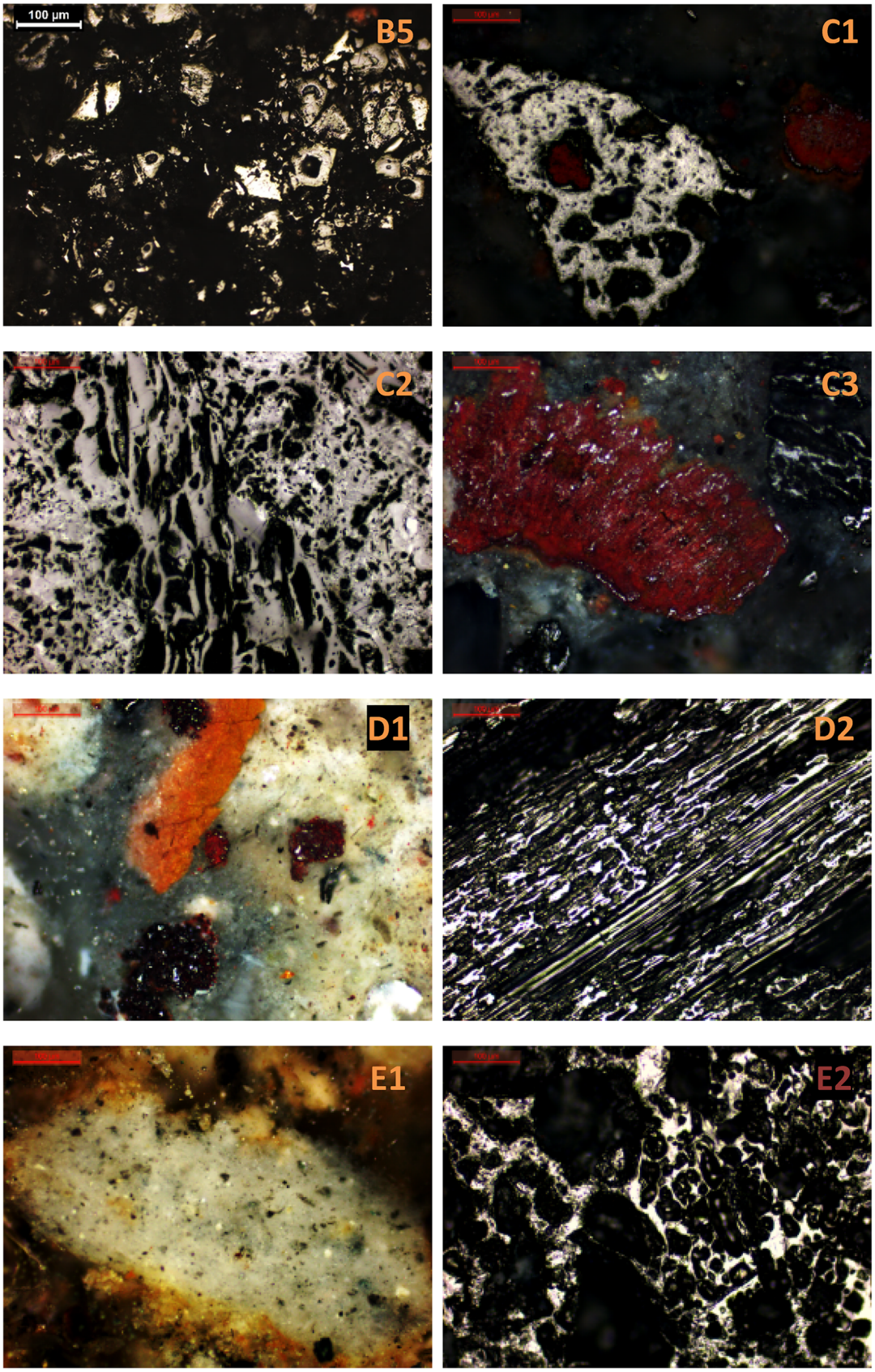

Fig. 2 continued

range, they get altered. However, below this range, oxidation did not ensue.

At 600 °C (Fig. 2**C1**–**C3**) temperature the sub-macerals of inertinite and heat affected macerals were very common in all density fractions. Vitrinite and liptinite were not seen in this temperature. In float fractions of the density of 1.3, the pores of fusinite became larger due to thermal alteration. In the float fractions of the densities of 1.4 and 1.5 heat affected macerals, fusinite and semifusinite were seen and the mineral matter occur either alone or associated with fusinite.

At 800 °C (Fig. 2**D1**–**D2**) and 1000 °C (Fig. 2**E1**–**E2**) temperatures, vitrinite and liptinite were not seen and metamorphosed inertinite occurs in all density. In the float fractions of the density of 1.5 gm/cm^3, the mineral matter is highest in amount (Table 3). Organic matter gradually decreased with density fraction.

Table 3 Petrographical variation of coal samples of different densities at different temperatures

T (°C)	Density	V_{mmf}	I_{mmf}	L_{mmf}	H_{mmf}	O_{mmf}	R_o	MM
HS		46.2	37.6	0.8	15.4	nf	1.36	7.2
200	F 1.3	52.4	29.4	2.1	16.1	nf	1.52	12.5
	F 1.4	43.0	36.4	1.7	18.9	nf	2.03	23.2
	F 1.5	36.9	41.7	0.8	20.6	nf	2.34	27.3
400	F 1.3	20.2	25.8	0.6	18.6	34.8	2.05	9.6
	F 1.4	24.6	32.0	nf	17.8	25.6	2.24	26.9
	F 1.5	28.7	38.9	nf	16.3	16.1	2.50	33.6
600	F 1.3	nf	48.8	nf	51.2	nf	nf	56.8
	F 1.4	nf	72.9	nf	27.1	nf	nf	87.1
	F 1.5	nf	84.0	nf	16.0	nf	nf	90.2
800	F 1.3	nf	63.5	nf	36.5	nf	nf	69.6
	F 1.4	nf	81.0	nf	19.0	nf	nf	71.6
	F 1.5	nf	86.0	nf	14.0	nf	nf	95.7
1000	F 1.3	nf	70.9	nf	29.1	nf	nf	73.9
	F 1.4	nf	73.1	nf	26.9	nf	nf	79.2
	F 1.5	nf	80.0	nf	20.0	nf	nf	98.1

HS Head Sample, *T* Temperature, *V* Vitrinite, *L* Liptinite, *I* Inertinite, *H* Heat affected, *O* Oxidised, R_o Mean reflectance of vitrinite, *MM* Mineral matter, *nf* Not found, *F* Float fraction, *mmf* mineral matter free basis

3.2.2 FTIR

Figure 3(**A**–**C**) represents the comparative FTIR spectra of the samples of different density with varying temperatures. The corresponding functional groups (Ibarra et al. 1996; Maity and Mukherjee 2006) of the bands present in each sample are tabulated in Table 4. The numbers of the peaks, coming from organic complex, decreased with increasing density. The −OH absorption in the range of 3419–3359 cm^{-1} due to the moisture absorbed in the residues during cooling process. The strong aliphatic and aromatic absorptions with C–O–C stretching and carbonyl (C=O) groups were present in low temperatures in all density fractions while at high temperature (>400 °C) some of these peaks were lost. Most of the peaks in FTIR spectra of coal between 1100 and 400 cm^{-1} are assigned to quartz and clay minerals such as kaolinite, illite and montmorillonite groups (Saikia et al. 2007) which increase with density.

The absence of vitrinite and liptinite macerals at >400 °C is also reflected by FTIR spectra where some of the peaks are lost in that temperature range (>400 °C). Therefore, it appears that with increasing temperature, the organic groups collapsed and macerals were oxidised. Oxidation at 400 °C has deleterious effects on coking properties and reduces the specific energy of steaming coal (Ignasiak et al. 1972; Fredericks et al. 1983). At >400 °C inertinite is seen in all density fractions whereas in FTIR spectra the C–O–C stretch is present with an aromatic nucleus (CH) and three to four adjacent H deformations as organic functional groups. In the higher density fraction, the mineral matter content is comparatively more (Table 4) which is also reflected in FTIR spectra.

Table 4 FTIR band positions found in samples

Sample name	Band position	Functional groups
F1.3; F1.4; F1.5	3419–3359	−OH stretching vibration
F1.3	3080–3035	Aromatic nucleus CH stretching vibration
F1.3	2975–2955	Aliphatic CH_3 asymmetric stretching vibration
F1.3; F1.4; F1.5	2925–2919	Aliphatic CH_2 asymmetric stretching vibration
F1.3; F1.4	1721–1695	Aromatic (carbonyl/carboxyl groups) (C=O)
F1.3; F1.4; F1.5	1615–1585	Aromatic nucleus (C=C)
F1.3; F1.4; F1.5	1460–1450	Aliphatic chains (CH_3, CH_2)
F1.3; F1.4; F1.5	1300–1000	Phenolic deformation C–O–C (stretching)
F1.3; F1.4	900–700	Aromatic bonds; $(C-H)_{ar}$ (out-plane bending)
F1.3; F1.4; F1.5	776–730	Aromatic nucleus (CH), three to four adjacent H deformations

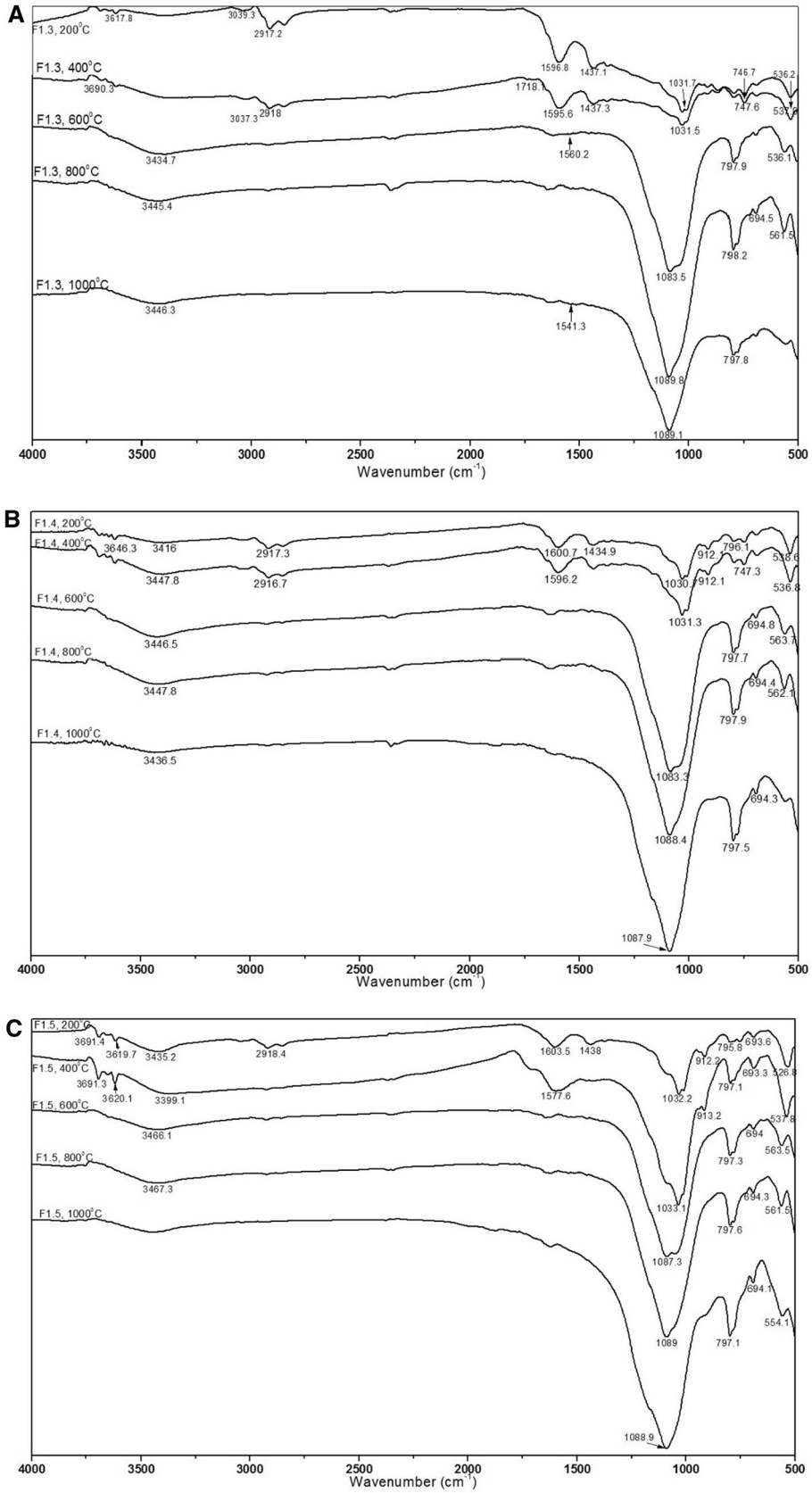

Fig. 3 FTIR spectra of coal samples of different density with varying temperature

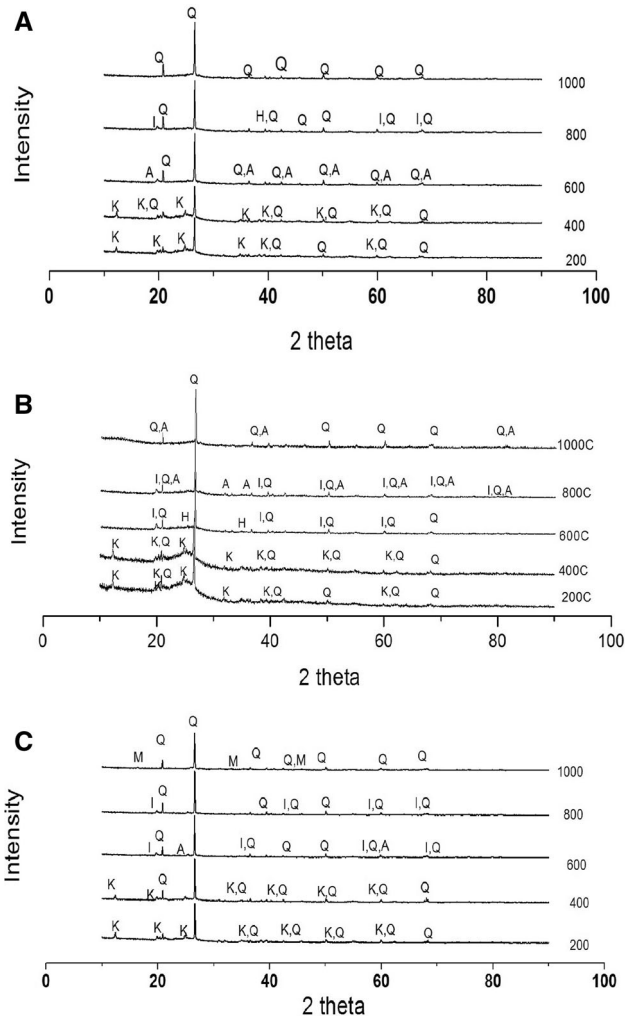

Fig. 4 XRD diffractograms of coal samples of different density and different temperature. **A** Float fraction of density 1.3. **B** Float fraction of density 1.4. **C** Float fraction of density 1.5. *K* kaolinite, *Q* Quartz, *I* Illite, *A* Andalusite, *M* Mullite

3.3 Mineral chemistry

The XRD analysis was performed on all the residues of different density fractions obtained from burning the coal samples at different temperatures. Figure 4 represents the comparative XRD diffractogram of same density fractions at different temperatures. It indicates evidently, the presence of kaolinite at low temperatures (≤400 °C), and illite, andalusite, mullite at high temperatures (>400 °C) whereas quartz was seen as the major mineral phase in all the samples of different density fractions at different temperatures. This indicates the mineral phase transformation with increasing temperature where the clay minerals were oxidised and form different type of oxides (Fig. 4**A**–**C**). The identification of minor minerals only by XRD in a multi component system like coal ashes is difficult due to the detection limits (normally at about 0.5%–1%) and peak overlapping (Mishra et al. 2016) and mullite peaks were only present at higher temperature (1000 °C) of float 1.5 density fraction. Hence, presence of mullite in higher density fraction indicates the higher concentration of mineral matter in that particular fraction.

4 Conclusions

This study provides a comprehensive view of the changes in organic structure with increasing temperature and helps to predict the structure of inertinite macerals. Coal undergoes appreciable physico-chemical changes when heated in the temperature range of 200–1000 °C during which, reacted molecules break along the weakest bonds, forming free radicals which subsequently recombine with other radicals or molecules to form more highly condensed species and volatile compounds. At ≤400 °C temperature, all the macerals are seen. The dominating macerals are vitrinite (telovitrinite, detrovitrinite) and inertinite (fusinite, semifusinite). The semifusinite has a low reflectivity but at 400 °C temperature, some of the vitrinite and inertinite macerals were oxidised. At >400 °C temperature the vitrinite and liptinite were not seen while porous inertinite was observed. In FTIR spectra, the absence of vitrinite and liptinite macerals in >400 °C is indicated by absence of their peaks at that temperature range. While inertinite survived, the other two macerals could not be seen at higher temperature. Therefore, it can be concluded that inertinite is most thermally stable maceral in coal. The clay minerals were oxidised at high temperature, which was revealed by XRD analysis.

Acknowledgements The authors are thankful to the Director, National Metallurgical Laboratory for permission to publish this work.

References

Acma HH, Yaman S, Kuçukbayrak S, Okutan H (2006) Investigation of the combustion characteristics of zonguldak bituminous coal using DTA and DTG. Energy Sour A 28:135–147

BIS (2003) Methods of test for coal and coke (2nd revision of IS: 1350). Part I, Proximate analysis. Bureau of Indian Standard, New Delhi, pp 1–29

Blanc P, Valisolalao J, Albrecht P, Kohut JP, Muller JF, Duchene JM (1991) Comparative geochemical study of three maceral groups from a high-volatile bituminous coal. Energy Fuels 5:875–884

Bouwman R, Freriks ILC (1980) Low temperature oxidation of a bituminous coal. IR spectroscopic study of samples from a coal pile. Fuel 59:315–322

Bustin RM, Guo Y (1999) Abrupt changes (jumps) in reflectance values and chemical compositions of artificial charcoals and inertinite in coals. Int J Coal Geol 38:237–260

Carlson GA (1992) Computer simulation of the molecular structure of bituminous coal. Energy Fuels 6:771–778

Chandra D (1992) Jharia coalfields. Geological Society of India, Bangalore, p 149

Cody GD, Davis A, Hatcher PG (1993) Physical structural characterization of bituminous coals: stress-strain analysis in the pyridine-dilated state. Energy Fuels 7:455–462

Creelman RA, Ward CR, Schumacher G, Juniper L (2013) Relation between coal mineral matter and deposit mineralogy in pulverized fuel furnaces. Energy Fuels 27:5714–5724

Diessel CFK (1992) Coal-bearing depositional systems. Springer, New York

Fox CS (1934) The Lower Gondwana coalfields of India. Mem Geol Surv India 59:386

Fredericks PM, Warbrooke P, Wilson MA (1983) Chemical changes during natural oxidation of a high volatile bituminous coal. Org Geochem 5(3):89–97

Giroux L, Charland JP, MacPhee JA (2006) Application of thermogravimetric Fourier transform infrared spectroscopy (TG−FTIR) to the analysis of oxygen functional groups in coal. Energy Fuels 20:1988–1996

Guo YT, Bustin RM (1998) Micro-FTIR spectroscopy of liptinite macerals in coal. Int J Coal Geol 36:259–275

Ibarra JV, Munoz E, Moliner R (1996) FTIR study of the evolution of coal structure during the coalification process. Org Geochem 24(6):725–735

Ignasiak BS, Clugston DM, Montgomery DS (1972) Oxidation studies on coking coal related to weathering. Part 2. The distribution of absorbed oxygen in the products resulting from the pyrolysis of slightly oxidised coking coal. Fuel 51:76–80

International Committee for Coal and Organic Petrology (1998) The new vitrinite classification (ICCP system 1994). Fuel 77:349–358

International Committee for Coal and Organic Petrology (2001) The new inertinite classification (ICCP system 1994). Fuel 80:459–471

International Committee of Organic and Coal Petrology (1963) International handbook of coal petrography, 2nd edn. Centre National de la Recherche, Paris

Kuehn DW, Davis A, Snyder RW, Starsinic M, Painter PC, Havens J, Koenig JL (1982) Application of FTIR and solid state 13C NMR to characterization of a set of vitrinite concentrates. ACS Div Fuel Chem 27(2):55–59

Larsen JW, Gurevich I, Glass AS, Stevenson DS (1996) A method for counting the hydrogen-bond cross-links in coal. Energy Fuels 10:1269–1272

Lowcnhaupt DE, Gray RJ (1980) The alkali-extraction test as a reliable method of detecting oxidized metallurgical coal. Int J Coal Geol 1:63–73

Mahajan OP, Komatsu M, Walker PL (1980) Low-temperature air oxidation of caking coals. 1. Effect on subsequent reactivity of chars produced. Fuel 59:3–10

Maity S, Mukherjee P (2006) X-ray structural parameters of some Indian coals. Curr Sci 91(3):337–377

Maroto-Valer MM, Taulbee DN, Andresen JM, Hower JC, Snape CE (1998) The role of semifusinite in plasticity development for a coking coal. Energy Fuels 12:1040–1046

Mastalerz M, Bustin RM (1993a) Electron-microprobe and micro-FTIR analysis applied tomaceral chemistry. Int J Coal Geol 24:333–345

Mastalerz M, Bustin RM (1993b) Variation in maceral chemistry within and between coals of varying rank: an electronic microprobe and micro-Fourier transform infrared investigation. J Microsc 171:153–166

Mastalerz M, Bustin RM (1995) Application of reflectance micro-Fourier transform infrared spectrometry in studying coal macerals: comparison with other Fourier transform infrared techniques. Fuel 74:536–542

Mastalerz M, Bustin RM (1996) Application of reflectance micro-Fourier transform infrared analysis to the study of coal macerals: an example from the late Jurassic to early Cretaceous coals of the Mist Mountain Formation, British Columbia, Canada. Int J Coal Geol 32:55–67

Mehta DRS, Murthy BRN (1957) A revision of the geology and coal resources of the Jharia Coalfield. Mem Geol Surv India 84:142

Meyer RA (1982) Coal structure. Academic Press, New York

Mishra V, Bhowmick T, Chakravarty S, Varma AK, Sharma M (2016) Influence of coal quality on combustion behaviour and mineral phases transformations. Fuel 186:443–455

Morga R (2010) Chemical structure of semifusinite and fusinite of steam and coking coal from the Upper Silesian Coal Basin (Poland) and its changes during heating as inferred from micro-FTIR analysis. Int J Coal Geol 84:1–15

Nakamura K, Takanohashi T, Iino M, Kumagai H, Sato M, Yokoyama S, Sanada YA (1995) Model structure of Zao Zhuang bituminous coal. Energy Fuels 9:1003–1010

Ozbas KE, Kok MV (2003) Effect of heating rate on thermal properties and kinetics of raw and cleaned coal samples. Energy Sour 25:33–42

Painter PC, Rhoads C (1981) Fourier transform infrared studies of coal oxidation. ACS Div Fuel Chem 26(1):35–38

Painter PC, Coleman MM, Jenkins RG, Walker PL (1978) FTIR study of acid-demineralised coal. Fuel 57:125–126

Painter PC, Snyder RW, Pearson DE, Kwong J (1980) FTIR study of the variation in the oxidation of a coking coal. Fuel 59:282–286

Painter PC, Snyder RW, Starsinic M, Coleman MM, Kuehn DW, Davis A (1981a) Concerning the application of FT-IR to the study of coal: a critical assessment of band assignments and the application of spectral analysis programs. Appl Spectrosc 35:475–485

Painter PC, Coleman MM, Snyder RW, Mahajan O, Komatsu M, Walker PL (1981b) Low temperature air oxidation of coking coals: FTIR studies. Appl Spectrosc 35:106–110

Pandolfo AG, Johns RB, Dyrkacz GR, Buchanan AS (1988) Separation and preliminary characterization of high-purity maceral group fractions from an Australian bituminous coal. Energy Fuels 2:657–662

Paul S, Chatterjee R (2011) Mapping of cleats and fractures as an indicator of in situ stress orientation, Jharia coalfield, India. Int J Coal Geol 88:113–122

Roberts MJ, Everson RC, Neomagus HWJP, Okolo GN, Niekerk DV, Mathews JP (2015) The characterisation of slow-heated inertinite- and vitrinite-rich coals from the South African coalfields. Fuel 158:591–601

Saikia BK, Boruah RK, Gogoi PK (2007) XRD and FTIR investigations of sub-bituminous Assam coals. Bull Mater Sci 30(4):421–426

Singh AL, Singh PK, Kumar A, Singh MP (2015) Demineralization of Rajmahal Gondwana coals by bacteria: revelations from X-ray diffraction (XRD) and Fourier transform infra-red (FTIR) studies. Energy Explor Exploit 33(5):755–767

Solomon PR (1981) Relation between coal structure and thermal decomposition products. Coal structure (Edited by Gorbaty M. L. and Ouchi K.). ACS Adv Chem 192:95–112

Solomon PR, Carangelo RM (1982) FTIR analysis of coal: I. Techniques and determination of hydroxyl concentrations. Fuel 61:663–669

Solomon PR, Carangelo RM (1988) FTIR analysis of coal: II. Aliphatic and aromatic hydrogen concentration. Fuel 67:949–959

Solum MS, Pugmire RJ, Grant DM (1989) Carbon-13 solid-state NMR of Argonne-premium coals. Energy Fuels 3:187–193

Sun SC (1954) Effects of oxidation of coals on their flotation properties. Trans AIME 6:396–401

Sun Q, Li W, Chen H, Li B (2003) The variation of structural characteristics of macerals during pyrolysis. Fuel 82:669–676

Taylor SR, Miller KJ, Deurbrouck AW (1980) Chemistry and Physics of Coal Utilization. In: Cooper BR, Petrakis L (eds) Topical Conference of the American Physical Society, American Institute of Physics, New York, p 344

Vasallo AM, Liu YL, Pang LSK, Wilson MA (1991) Infrared spectroscopy of coal maceral concentrates at elevated temperatures. Fuel 70:635–639

Vassileva CG, Vassilev SV (2006) Behaviour of inorganic matter during heating of Bulgarian coals 2. Subbituminous and bituminous coals. Fuel Process Technol 87:1095–1116

Walker R, Mastalerz M (2004) Functional group andindividualmaceralchemistry of high volatile bituminouscoals from southern Indiana: controls on coking. Int J Coal Geol 58:181–191

Wang J, Du J, Chang L, Xie K (2010) Study on the structure and pyrolysis characteristics of Chinese western coals. Fuel Process Technol 91:430–433

White A, Davies MR, Jones S (1989) Reactivity and characterization of coal maceral concentrates. Fuel 68:511–519

Wu D, Liu G, Sun R, Xiang F (2013) Investigation of structural characteristics of thermally metamorphosed coal by FTIR spectroscopy and X-ray diffraction. Energy Fuels 27:5823–5830

Xie KC, Zhang YF, Li CZ, Ling DQ (1991) Pyrolysis characteristics of macerals separated from a single coal and their artificial mixture. Fuel 70:474–479

Xuguang S (2005) The investigation of chemical structure of coal macerals via transmitted-light FT-IR microspectroscopy. Spectrochim Acta A 62:557–564